Proceedings of the 21st ICSMGE, Vienna, Austria, 14 – 19 June 2026. Pistrol, Adam & Schweiger (eds.)
Published by: ÖGG, Austrian Society for Geomechanics, Salzburg, Austria, ISBN 978-3-9503898-4-5
https://doi.org/10.53243/ICSMGE2026-719

Bentonite-based barrier systems for the control of PFAS-contaminated leachates

Nicolò Guarena, Andrea Dominijanni, Mario Manassero
Department of Structural, Geotechnical and Building Engineering, Polytechnic University of Turin, Italy, nicolo.guarena@polito.it

Andriy Yaroshchuk
ICREA & Department of Chemical Engineering, Polytechnic University of Catalonia, Spain

ABSTRACT: The widespread presence of per- and poly-fluoroalkyl substances (PFAS) in waste disposal facilities has raised concerns about the effectiveness of landfill lining systems in limiting the migration of such a class of emerging contaminants to the groundwater, with particular regard to engineered bentonite-based barriers that are increasingly being accepted as a replacement of traditional compacted clay liners. With the aim to cover the current knowledge gap on the relation between the semipermeable membrane behavior of bentonites and the transport of PFAS, this paper illustrates the experimental evidence that emerged from a multi-stage membrane test, conducted on a natural Wyoming bentonite in equilibrium with aqueous solutions of sodium chloride (NaCl) and sodium perfluorooctanoate ($C_8F_{15}NaO_2$). NaCl was used as the background (dominant) salt, and its concentration at the contaminated-solution side of the bentonite specimen was varied stepwise in the 1 to 100 mM range, in such a way simulating a broad spectrum of ionic strengths that may be encountered in field scenarios. In contrast, the $C_8F_{15}NaO_2$ concentration at the contaminated-solution side was kept constantly equal to 0.1 mM, which was low enough for $C_8F_{15}NaO_2$ to be regarded as a tracer contaminant and the ionic selectivity of the tested bentonite specimen to be only controlled by the NaCl concentration. The hydraulic head difference, which built up across the bentonite specimen under closed-system boundary conditions, was measured in parallel with the concentrations of sodium, chloride, and perfluorooctanoate ions in the liquid samples, which were regularly collected from the outlet reservoir. The obtained test results highlighted a correlation between the reflection coefficient, which was calculated as a function of the measured hydraulic head difference, and the mass flux of perfluorooctanoate ions through the bentonite specimen, with a change in the latter mass flux of almost one order of magnitude for the investigated NaCl concentration range.

KEYWORDS: Active clays, coupled phenomena, emerging contaminants, PFAS, waste disposal.

1 INTRODUCTION

Per- and poly-fluoroalkyl substances (PFAS) are a group of emerging contaminants, which include more than 4,000 fluorinated organic compounds that have been extensively used, since the middle of the past century, for the production of a large variety of consumer goods due to their hydrophobic and oleophobic properties, their ability to behave as surfactants, and their exceptional resistance to decomposition by heat and chemical attack. Due to the growing awareness of the adverse effects of PFAS on human health and ecosystems, manufacturing of certain classes of PFAS has started to be banned or restricted in many jurisdictions since the late 1990s, and in parallel the scientific community has been called to develop remediation strategies for the reclamation of PFAS-contaminated sites, most notably military bases, airports, fire-fighting training facilities, wastewater treatment plants, and industrial plants where these chemicals were synthesized or used as processing aids.

Well established *in-situ* remediation techniques for the removal of water-miscible contaminants (e.g., pump and treat) were found not to be effective in the case of soils contaminated by PFAS, due to the extremely slow kinetics of desorption associated with the hydrophobic interaction of such compounds with the organic matter of soils (Kato et al. 2025). Additional phenomena undermining the effectiveness of *in-situ* remediation techniques are the preferential accumulation of PFAS at the air-water interface in the vadose zone (Das et al. 2024; Stults et al. 2024; Alam & Farid 2025), which is responsible for the peak in the PFAS leaching that is commonly observed in response to fluctuations of the water table, and the retention at the oil-water interface (Silva et al. 2019), which can be of concern in multi-phase systems characterized by the presence of water-immiscible organic liquids.

As an alternative to *in-situ* remediation, a number of *ex-situ* remediation strategies have been proposed in the recent past (Barth et al. 2021; Quinnan et al. 2022), involving excavation of the PFAS-contaminated soil and treatment to reduce the concentration of these harmful chemicals (e.g., soil washing, bioremediation, thermal treatment, and phytoremediation) or to restrict their mobility through addition of binding and/or sorbing agents. In the context of *ex-situ* remediation, permeable geocomposites amended with activated carbon or ion exchange resins, which have recently been introduced in the geosynthetics industry, are a promising solution for the reuse of PFAS-contaminated soils to construct earthen dams, road embankments, or any other geotechnical structures (Kato et al. 2023; Niewerth et al. 2023).

Despite its attractiveness for the implementation of more sustainable practices in civil engineering, the *ex-situ* treatment or reuse of the excavated soil is unfeasible in most cases due to possible conflicts with the environmental legislation in force, risks for the operators involved in the management of the contaminated matrix, time constraints, as well as limitations associated with the high costs and energy demand of these technical solutions. Therefore, landfilling has been the most widely adopted practice so far to manage PFAS-contaminated soils. Besides the disposal of contaminated materials resulting from the remediation activities, landfills have been for decades the final repository of consumer goods (e.g., stain-resistant coatings and food packaging) and industrial byproducts containing PFAS, so that the measured concentration of these emerging contaminants in landfill leachates is typically higher than that measured in other environmental media (Bouazza, 2021; Zhang et al. 2023).

Since waste disposal facilities are recognized as potential sources of PFAS contamination for surface water and groundwater, concerns are being raised by landfill owners, regulators, and geoenvironmental engineers about the ability of landfill lining systems, which comprise a low-permeability mineral layer overlain by a polymeric geomembrane, to restrict the migration of PFAS towards the environmental receptors (Rowe & Barakat 2021). Linear low-density polyethylene (Di Battista et al. 2020), thermoplastic polyurethane and polyvinyl

chloride alloyed with ketone ethylene ester (Rowe et al. 2023), and high-density polyethylene geomembranes (Ahmad et al. 2024) were found to be excellent barriers against PFAS migration when devoid of defects because of the very low values of the diffusion coefficient, typically from three to five orders of magnitude lower compared to other volatile organic compounds of concern (e.g., benzene and toluene). The preferential migration pathways of PFAS through landfill composite liners are therefore the geomembrane defects (e.g., punctures, tears, and defective seams), which are generated during the construction of the lining system and the landfilling operations (Guarena et al. 2023, 2024). Under such conditions, the ability of the underlying mineral layer to maintain both a low hydraulic conductivity and a high attenuation capacity when permeated with PFAS-contaminated leachates is of the utmost importance, and accordingly this latter issue has already been the subject of experimental research (Li et al. 2015; Barakat et al. 2024; Mikhael et al. 2025a, 2025b).

The use of engineered bentonite-based barriers (e.g., geosynthetic clay liners and bentonite-amended soil liners) in place of traditional compacted clay liners can further enhance the containment performance of landfill lining systems as a result of the semipermeable membrane behavior of the bentonite component, which is able to partially exclude charged (ionic) solutes from pores that are freely accessible to the water molecules (Tang et al. 2014, 2015; Malusis et al. 2015, 2020; Musso et al. 2017; Dominijanni et al. 2018; Sample-Lord & Shackelford 2018; Shackelford et al. 2019; Manassero, 2020; Guarena et al. 2022, 2025a; Mazzieri & Bernardo 2023; Fritz et al. 2025). The potential benefit associated with the ionic selectivity of engineered bentonite-based barriers is expected to be particularly relevant in the case of perfluoroalkyl acids (PFAA), which almost entirely dissociate into their constituent ions under near-neutral pH conditions and, for such a reason, are greatly affected by the electrostatic interactions with the negatively charged mineral phase.

Since there is currently a lack of evidence on the relation between the semipermeable membrane behavior of bentonites and the transport of PFAA, this paper aims to present the results of a multi-stage membrane test, which was conducted on a natural Wyoming bentonite in equilibrium with aqueous solutions of sodium chloride (NaCl) and sodium perfluorooctanoate ($C_8F_{15}NaO_2$). The NaCl concentration at the contaminated-solution side was increased stepwise during the test, so as to progressively diminish the extent of ionic selectivity of the bentonite specimen, while the $C_8F_{15}NaO_2$ concentration, which was low enough for $C_8F_{15}NaO_2$ to be regarded as a tracer contaminant, was kept constant. The obtained test results, which highlight a remarkable dependence of the mass flux of perfluorooctanoate ions on the reflection coefficient of the tested bentonite, allow for a more informed use of bentonite-based containment barriers by engineering practitioners.

2 MATERIALS AND METHODS

2.1 *Bentonite and salt solutions*

The powdered bentonite tested in this study, which is distributed by The Clay Minerals Society (Chantilly, Virginia, USA) under the name "Na-rich montmorillonite", belongs to the geological formation of the Newcastle (County of Crook, Wyoming, USA), comprising shales, marls, and argillaceous sandstones (Moll, 2001). Interpretation of the X-ray diffraction patterns, recorded on the "as-shipped" material, yielded a mineralogical composition primarily consisting of smectite (75%), with feldspar (16%) and quartz (8%) being present as the main impurities (Chipera & Bish 2001). The cation exchange capacity, which was measured through the ammonia-electrode method, resulted to be equal to 85 meq/100g (Borden & Giese 2001).

The salt solutions were prepared with sodium chloride (ACS reagent, purity ≥ 99%, purchased from Merck KGaA, Darmstadt, Germany) and sodium perfluorooctanoate (purity ≥ 97%, purchased from Santa Cruz Biotechnology, Heidelberg, Germany), which is the sodium salt of perfluorooctanoic acid (PFOA). The choice of $C_8F_{15}NaO_2$ as a representative compound of the PFAA class was motivated by the widespread presence of PFOA in landfill leachates, the availability of literature studies on the basic physico-chemical properties of PFOA (e.g., critical micelle concentration and aqueous-phase diffusion coefficient), and the possibility to measure the aqueous-phase concentration of PFOA with a level of accuracy and precision that is adequate for the experimental activity. Distilled water, which was obtained by boiling tap water and condensing the steam into a sterilized container (water distiller DESA 0081, produced by Vidrio Industrial Pobel, Madrid, Spain), was used as both the solvent for the preparation of the testing solutions and the dialysate for the bentonite purification. The concentrations of sodium (Na^+), potassium (K^+), calcium (Ca^{2+}), and magnesium ions (Mg^{2+}) in the liquid samples that were collected during the multi-stage membrane test were measured using the inductively coupled plasma mass spectrometry (U.S. EPA, 2014), whereas the concentrations of chloride ions (Cl^-) were measured using the ion chromatography (U.S. EPA, 2007). High-performance liquid chromatography, coupled with triple quadrupole mass spectrometry, was adopted to measure the concentrations of perfluorooctanoate ions ($C_8F_{15}O_2^-$).

2.2 *Testing apparatus*

The impact of the ionic selectivity of the natural Wyoming bentonite on the transport of PFOA was investigated by means of the laboratory apparatus developed by Dominijanni et al. (2018). The primary components of the testing apparatus include an osmotic cell, three pressure transducers, a flow-pump accumulator, and a displacement transducer (i.e., a linear variable differential transformer, LVDT).

The osmotic cell consists of a stainless steel oedometer (70-mm inner diameter), where the top piston and the bottom pedestal are endowed with three drainage lines. The two peripheral lines allow different salt solutions to circulate at the boundaries of the clay specimen, so that an electro-chemical potential gradient is established across the specimen and is maintained constant throughout the testing stages. The central line is connected to the differential pressure transducer (UNIK 5000 Silicon Pressure Sensor, accuracy ± 0.1% FS BSL, produced by GE Measurement & Control, Billerica, Mass., USA), which enables the difference in hydraulic head to be measured across the specimen. The hydraulic head in the circulation loops through the top piston and bottom pedestal is monitored by two additional relative pressure transducers. The flow-pump accumulator consists of a dual-carriage syringe pump (Model 33 Twin Syringe Pump, produced by Harvard, Holliston, Mass., USA) and two stainless steel actuators (ADN-50-200-A-P-A-S2, produced by Festo, Assago, Italy), which simultaneously inject and withdraw the same volume of solution from both the top and bottom boundaries to prevent any liquid flux from occurring through the specimen. The displacement transducer (Series TR-0025, repeatability 0.002 mm, produced by Novotechnik, Southborough, Mass., USA) allows the specimen height to be monitored during both the preliminary stage (i.e., compaction-swelling stage) and the membrane testing stages, when the specimen volume is maintained constant.

The 6-mm-thick, porous ceramic filters, which were originally used by Dominijanni et al. (2018) in a sandwich-type arrangement (i.e., filter-clay-filter) to confine the tested specimen, were replaced by porous stainless-steel filters (stainless steel 316 L, avg. pore size 5 μm, disc diameter 69.85 mm, thickness 0.71 mm, produced by Mott Corporation, Farmington, Conn., USA). In such a way, the diffusive resistance of the filters was negligible compared to that of the clay specimen, and therefore the mass-transfer limitations associated with the filters could be ignored in the interpretation of the membrane test results (Glaus et al. 2008; Yaroshchuk & Van Loon 2008; Yaroshchuk et al. 2008, 2009; Sample-Lord & Shackelford 2018; Guarena et al. 2025a).

2.3 *Specimen preparation*

Prior to membrane testing, the natural Wyoming bentonite was subjected to the dialysis procedure, which was described by Sample-Lord & Shackelford (2016) and further developed by Guarena et al. (2025b), to remove the excess soluble salts that are naturally contained in the bentonite pores, and ultimately to prevent them from interfering with the experiment. According to such a conditioning procedure, a total amount of 60 g (oven-dried mass) of powdered bentonite was uniformly distributed inside four different dialysis tubes, which were made of regenerated cellulose (flat width 76 mm, MWCO 14 kDa, purchased from Merck KGaA, Darmstadt, Germany), sealed via clamps at both ends of the tubes, and then placed inside a glass jar, which was filled with 7 L of the dialysate (i.e., distilled water). The dialysate was continuously stirred and replaced daily with fresh distilled water, in order to maintain a solute concentration gradient across the membrane tubing. The dialysis procedure, which lasted 34 days, was interrupted when the incremental change in the dialysate electrical conductivity between two consecutive replacements was negligible, and the dialyzed bentonite, after oven-drying at 105 °C, was gently ground and sifted through an ASTM No. 200 mesh sieve.

A known amount of treated material (dry mass equal to 23.61 g) was dusted inside the oedometer ring, the top piston was brought into contact with the upper face of the specimen, and distilled water was supplied from the bottom pedestal to saturate the bentonite. During the saturation stage, which was conducted under a controlled hydraulic gradient of 1000, the specimen was allowed to swell freely in the axial direction to a specified height (10.2 mm), which corresponded to a void ratio, e, equal to 3.396 and a water content, w, equal to 128.4%. After reaching the desired height, the top piston was locked in place to prevent any further volumetric strain from occurring, and saturation was continued for a period of 52 day, corresponding to approximately 16 Pore Volumes of Flow, to obtain a steady-state value of the hydraulic conductivity, k ($k \sim 2 \cdot 10^{-11} \div 3 \cdot 10^{-11}$ m/s). Upon completion of the bentonite saturation, the drainage lines were connected to the ports of the osmotic cell and a NaCl solution with a concentration of 1 mM was continuously infused at both the top and bottom specimen boundaries for a period of 10 days.

2.4 *Testing procedures*

The multi-stage membrane test was carried out by circulating different salt solutions through the top and bottom porous filters at a circulation rate of 0.05 mL/min, which was recognized to be sufficiently fast for perfect-flushing boundary conditions to be hypothesized in the interpretation of the test results and, at the same time, sufficiently slow for the ionic mass fluxes to be measured through the bentonite specimen (Dominijanni et al. 2018; Guarena et al. 2025a). The $C_8F_{15}NaO_2$ concentration of the solution injected into the top boundary and the NaCl concentration of the solution injected into the bottom boundary were maintained constantly equal to 0.1 and 1 mM, respectively, for the entire duration of the membrane test, while the NaCl concentration of the solution injected into the top boundary was increased stepwise from 1 to 100 mM (Table 1).

Table 1. Values of the measured concentration of $C_8F_{15}O_2^-$ ions, calculated mass flux of $C_8F_{15}O_2^-$ ions, measured hydraulic head difference, imposed osmotic pressure difference, and calculated global reflection coefficient for the multi-stage membrane test conducted on the natural bentonite.

		Stage 1	Stage 2	Stage 3	Stage 4	Stage 5	Stage 6	Stage 7
$c_{NaCl,T}$	(mM)	1	2	5	10	20	50	100
$c_{NaPFO,T}$	(mM)	0.1	0.1	0.1	0.1	0.1	0.1	0.1
$c_{NaCl,B}$	(mM)	1	1	1	1	1	1	1
$c_{NaPFO,B}$	(mM)	0	0	0	0	0	0	0
$\left(c_{PFO,B}^{exit}\right)_{ss}$	(μM)	0.38	0.57	0.84	0.97	1.28	1.50	1.57
$\left(J_{PFO}\right)_{ss}$	($\times 10^{-10}$ mol·m^{-2}·s^{-1})	0.823	1.234	1.819	2.100	2.772	3.248	3.400
$\left(\Delta h\right)_{ss}$	(m)	-	0.25	0.5	0.75	1.15	1.55	2.3
$\Delta\Pi$	(kPa)	0.50	5.45	20.33	45.11	94.69	243.42	491.30
ω_g	(-)	-	0.450	0.241	0.163	0.119	0.062	0.046

Note: $c_{NaCl,T}$ and $c_{NaCl,B}$, NaCl concentrations of the solutions injected into the top and bottom boundaries, respectively; $c_{NaPFO,T}$ and $c_{NaPFO,B}$, $C_8F_{15}NaO_2$ concentrations of the solutions injected into the top and bottom boundaries, respectively; $\left(c_{PFO,B}^{exit}\right)_{ss}$, steady-state concentration of $C_8F_{15}O_2^-$ ions of the solutions withdrawn from the bottom boundary; $\left(J_{PFO}\right)_{ss}$, steady-state mass flux of $C_8F_{15}O_2^-$ ions through the bentonite specimen; $\left(\Delta h\right)_{ss}$, steady-state hydraulic head difference across the bentonite specimen; $\Delta\Pi$, osmotic pressure difference across the bentonite specimen; ω_g, global reflection coefficient at steady state.

While the hydraulic head difference, Δh, induced across the specimen was continuously monitored at time increments of 120 s, samples of the solutions exiting from the bottom specimen boundary were collected for the measurement of the concentrations of Na^+, K^+, Ca^{2+}, Mg^{2+}, Cl^-, and $C_8F_{15}O_2^-$ ions when the flow-pump system was briefly halted to refill the hydraulic actuators, which have a runtime of 72 h before the plunger barrel reaches the end of the actuator housing at a circulation rate of 0.05 mL/min.

When steady-state conditions were deemed to be achieved for each testing stage, the global reflection coefficient, ω_g, was calculated as follows:

$$\omega_g = \frac{\gamma_w \left(\Delta h\right)_{ss}}{\Delta \Pi} \quad (1)$$

where γ_w is the water unit weight (γ_w = 9.81 kN/m^3), $\left(\Delta h\right)_{ss}$ is the difference in hydraulic head, which is measured across the specimen under steady-state conditions, and $\Delta \Pi$ is the difference in osmotic pressure of the external bulk solutions, which are in thermodynamic equilibrium with the porous medium at its boundaries.

The steady-state mass flux of $C_8F_{15}O_2^-$ ions, $\left(J_{\mathrm{PFO}}\right)_{ss}$, through the bentonite specimen was determined for each testing stage as follows:

$$\left(J_{\mathrm{PFO}}\right)_{ss} = \frac{v_w}{A} \cdot \left(c^{exit}_{\mathrm{PFO},B}\right)_{ss} \quad (2)$$

where v_w is the circulation rate imposed by the flow-pump system (v_w = 0.05 mL/min), A is the inner cross-sectional area of the oedometer cell (A = 38.48 cm^2), and $\left(c^{exit}_{\mathrm{PFO},B}\right)_{ss}$ is the steady-state concentration of $C_8F_{15}O_2^-$ ions of the solutions withdrawn from the bottom specimen boundary.

3 RESULTS AND DISCUSSION

The hydraulic head difference, which was measured across the bentonite specimen, and the concentration of $C_8F_{15}O_2^-$ ions of the solutions exiting from the bottom specimen boundary, which were collected during the refilling phases of the hydraulic actuators, are shown in Figure 1 and Figure 2, respectively, as a function of time.

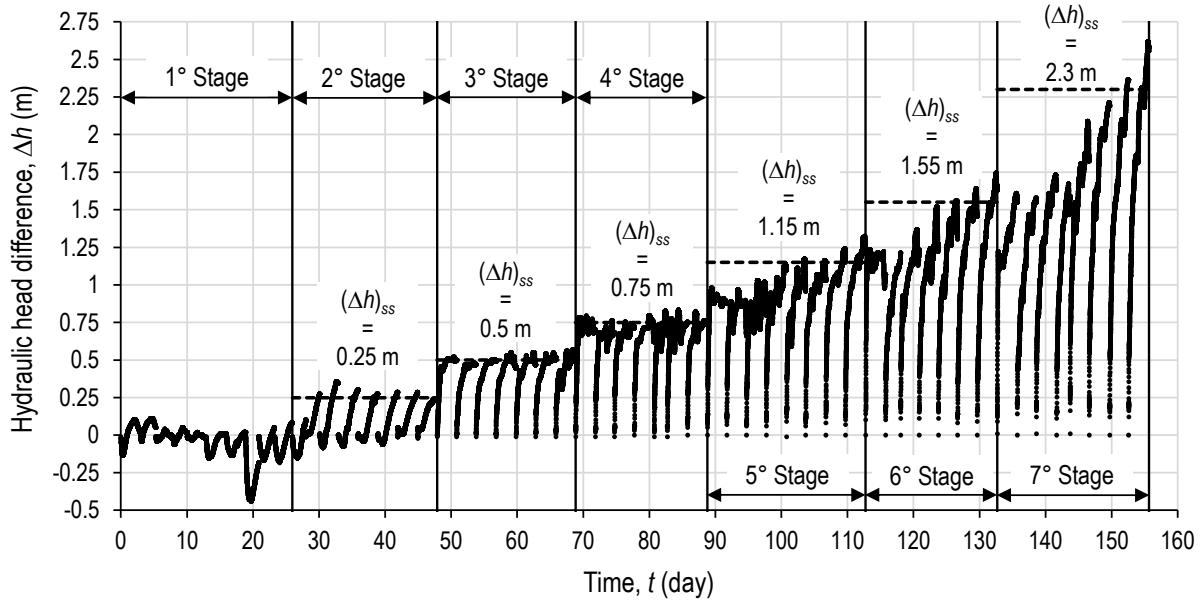

Figure 1. Hydraulic head difference, Δh, as a function of time during the multi-stage membrane test conducted on the natural Wyoming bentonite.

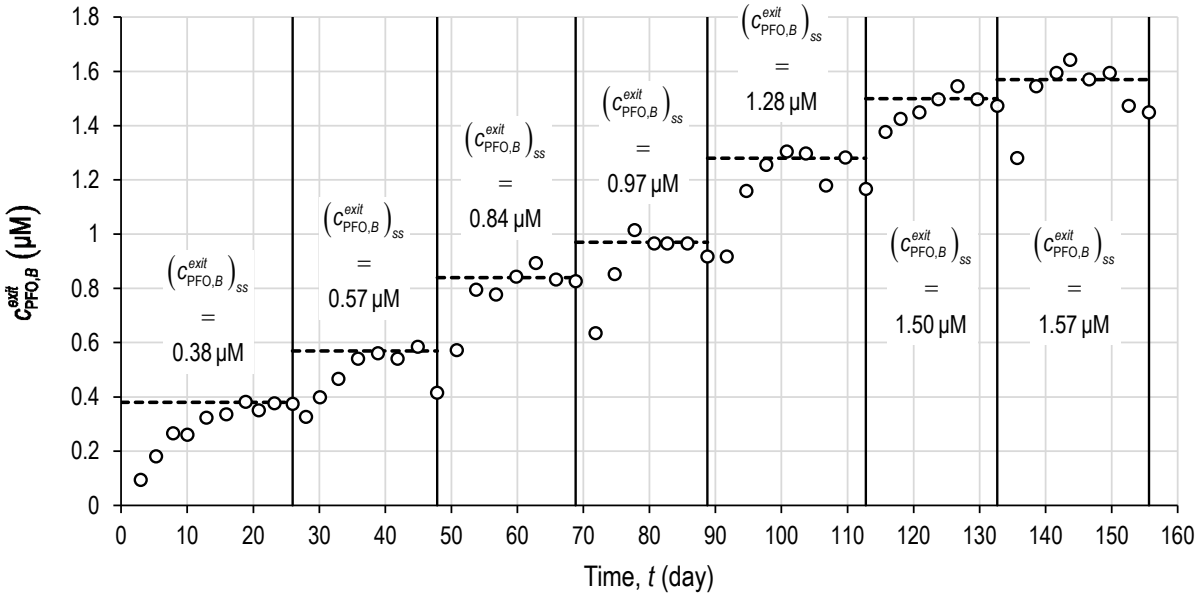

Figure 2. Concentration of $C_8F_{15}O_2^-$ ions of the solutions exiting from the bottom specimen boundary, $c^{exit}_{\mathrm{PFO},B}$, as a function of time during the multi-stage membrane test conducted on the natural Wyoming bentonite.

The estimation of the steady-state values of both Δh and $c_{PFO,B}^{exit}$, which are reported in Table 1, was based on the observation of the overall experimental trends over time, whereby steady-state conditions were found to be achieved after approximately two-three weeks from the beginning of each testing stage. Stage No. 7 was the only exception, since the measured hydraulic head difference steadily increased without tending to a distinct horizontal asymptote, and therefore the value of ω_g for Stage No. 7 should be regarded as potentially affected by an estimation error.

The obtained test results allow the impact of the semipermeable membrane behavior of the bentonite specimen on the transport of $C_8F_{15}O_2^-$ ions to be appreciated. Upon an increase in the concentration of NaCl as the dominant salt at the contaminated-solution side, the extent of ionic partitioning in the bentonite pores is diminished and, accordingly, the measured global reflection coefficient decreases to negligibly small values at the highest concentrations of the dominant salt. Such a decrease in the exclusion of anionic (negatively charged) species from the bentonite pores correlates with a reduced ability of the bentonite specimen to restrict the diffusive transport of $C_8F_{15}O_2^-$ ions (Shackelford & Moore 2013; Malusis et al. 2015), which reflects on the increase in the measured mass flux of $C_8F_{15}O_2^-$ ions under the same concentration gradient of the tracer contaminant ($C_8F_{15}NaO_2$). The evidence emerged from the experimental activity is further stressed in Figure 3, which highlights the inverse correlation between the mass flux of $C_8F_{15}O_2^-$ ions and the global reflection coefficient.

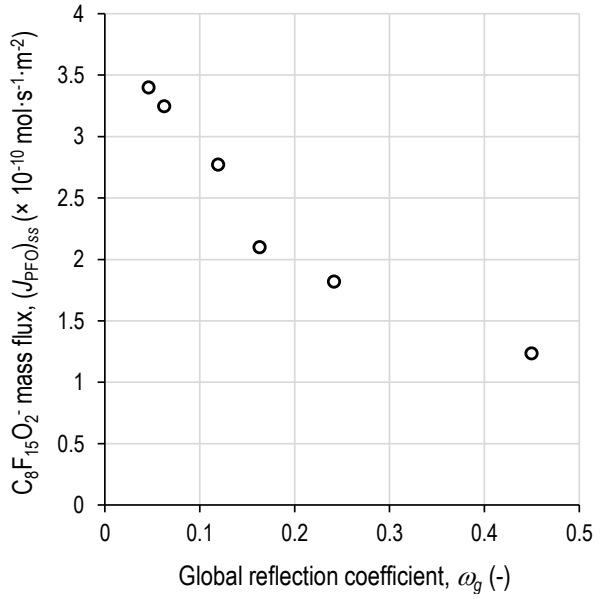

Figure 3. Steady-state mass flux of $C_8F_{15}O_2^-$ ions, $(J_{PFO})_{ss}$, through the bentonite specimen as a function of the global reflection coefficient, ω_g.

4 CONCLUSIONS

A multi-stage membrane test was carried out on a natural Wyoming bentonite, preliminarily treated via dialysis for the removal of the excess soluble salts, with a view to characterizing the coupling between the ionic selectivity of the tested specimen, which was controlled by the concentration of NaCl as the dominant salt in the testing solutions, and the transport of $C_8F_{15}NaO_2$ at tracer concentrations. Indeed, considering the high values of the acid dissociation constant (i.e., low values of pK_a), chemical compounds belonging to the PFAA class mostly dissociate into their constituent ions under pH conditions of environmental concern (pH = 5.0 – 9.0), giving rise to anions that interact with the mineral phase through repulsive electrostatic forces. While these repulsive forces undermine the ability of containment barriers comprising natural bentonites to retard the breakthrough of PFAA (Li et al. 2015; Barakat et al. 2024), the semipermeable properties arising from the anion exclusion mechanism in the bentonite pores potentially restrict the steady-state diffusive transport of PFAA to a greater extent than barriers comprising non-active clays.

The concentration gradient of $C_8F_{15}NaO_2$ across the bentonite specimen was kept constant throughout the multi-stage membrane test, which lasted 156 days, whereas the concentration of NaCl at the contaminated-solution side was increased stepwise in the 1 to 100 mM range. Upon an increase in the NaCl concentration, the measured global reflection coefficient decreased from a maximum value of 0.450 to a minimum value of 0.046. In parallel with the decrease in the reflection coefficient, the measured mass flux of $C_8F_{15}O_2^-$ ions increased from $0.823 \cdot 10^{-10}$ to $3.400 \cdot 10^{-10}$ mol·m^{-2}·s^{-1}, thus providing the first experimental evidence, at the time of writing, of the influence of the semipermeable membrane behavior of engineered bentonite-based barriers on the transport of PFAA at tracer concentrations.

The obtained evidence further suggests caution in the use of additives (e.g., activated carbon, ion exchange resin, and quaternary ammonium) aimed at enhancing the adsorption capacity of bentonites towards PFAS. Although mixing with additives, which are able to bond with PFAS, improves the retention of such a group of emerging contaminants by bentonites (Khodabakhshloo et al. 2021; Wang et al. 2021; Mikhael et al. 2025b), the bentonite modification can promote a flocculation of the microstructure, a reduction in the fraction of the specific surface area that electrostatically interacts with the ionic species in the pore solution, and eventually a loss of the long-term benefits associated with the semipermeable membrane behavior (Mazzieri et al. 2010).

5 ACKNOWLEDGEMENTS

The authors would like to thank Eni Rewind S.p.A. (Milan, Italy) for their financial support of this study.

6 REFERENCES

Ahmad, A., Tian, K., Tanyu, B., and Foster, G.D. 2024. Sorption and diffusion of per-polyfluoroalkyl substances (PFAS) in high-density polyethylene geomembranes. *Waste Management* 174, 15-23.

Alam, M.K., and Farid, A. 2025. Coupled PFAS transport and seepage models to evaluate retardation due to air-water-interface adsorption. *Proc. Geo-EnvironMeet 2025*, Louisville, 24-33.

Barakat, F.B., Rowe, R.K., Patch, D., and Weber, K. 2024. Transport parameters for PFOA and PFOS migration through GCL's and composite liners used in landfills. *Geotextiles and Geomembranes* 52(4), 762-772.

Barth, E., McKernan, J., Bless, D., and Dasu, K. 2021. Investigation of an immobilization process for PFAS contaminated soils. *Journal of Environmental Management* 296, 113069.

Borden, D., and Giese, R.F. 2001. Baseline studies of The Clay Minerals Society source clays: cation exchange capacity measurements by the ammonia-electrode method. *Clays and Clay Minerals* 49(5), 444-445.

Bouazza, A. 2021. Interaction between PFASs and geosynthetic liners: Current status and the way forward. *Geosynthetics International* 28(2), 214-223.

Chipera, S.J., and Bish, D.L. 2001. Baseline studies of The Clay Minerals Society source clays: powder X-ray diffraction analyses. *Clays and Clay Minerals* 49(5), 398-409.

Das, T.K., Han, Z., Banerjee, S., Raoelison, O.D., Adeleye, A.S., and Mohanty, S.K. 2024. PFAS release from the subsurface and

capillary fringe during managed aquifer recharge. *Environmental Pollution* 343, 123166.

Di Battista, V., Rowe, R.K., Patch, D., and Weber, K. 2020. PFOA and PFOS diffusion through LLDPE and LLDPE coextruded with EVOH at 22 °C, 35 °C, and 50 °C. *Waste Management* 117, 93-103.

Dominijanni, A., Guarena, N., and Manassero, M. 2018. Laboratory assessment of semi-permeable properties of a natural sodium bentonite. *Canadian Geotechnical Journal* 55(11), 1611-1631.

Fritz, C.J., Scalia, J., and Shackelford, C.D. 2025. Limiting membrane behavior of compacted sand-bentonite mixture. *Journal of Rock Mechanics and Geotechnical Engineering* 17(4), 2433-2444.

Glaus, M.A., Rossé, R., Van Loon, L.R., and Yaroshchuk, A.E. 2008. Tracer diffusion in sintered stainless steel filters: measurement of effective diffusion coefficients and implications for diffusion studies with compacted clays. *Clays and Clay Minerals* 56(6), 677-685.

Guarena, N., Dominijanni, A., and Manassero, M. 2022. The role of diffusion induced electro-osmosis in the coupling between hydraulic and ionic fluxes through semipermeable clay soils. *Soils and Foundations* 62(4), 101177.

Guarena, N., Dominijanni, A., and Manassero, M. 2023. Contaminant transport through landfill composite liners due to geomembrane defects. *Proc. 12th International Conference on Geosynthetics*, Rome, 1413-1422.

Guarena, N., Dominijanni, A., and Manassero, M. 2024. Theoretical assessment of the advective-diffusive transport of contaminants through landfill composite liners. *Proc. 18th European Conference on Soil Mechanics and Geotechnical Engineering*, Lisbon, 2939-2943.

Guarena, N., Dominijanni, A., and Manassero, M. 2025a. Reflection coefficient of a natural sodium bentonite in aqueous mixed electrolyte solutions: positive and negative anomalous osmosis. *Canadian Geotechnical Journal* 62(1), 1-18.

Guarena, N., Mazzieri, F., Dominijanni, A., Fratalocchi, E., and Manassero, M. 2025b. Laboratory procedures for the modification of soluble and exchangeable cations of geosynthetic clay liners. *Proc. 8th European Conference on Geosynthetics*, Lille, accepted for publication.

Kato, T., Takai, A., Zhang, Y., Gathuka, L.W., Katsumi, T., and Kinoshita, Y. 2023. Geosynthetic sorption sheet - Another function of geosynthetics? *Proc. 12th International Conference on Geosynthetics*, Rome, 1527-1533.

Kato, T., Yoshimura, H., Takai, A., Tanaka, S., Li, W., and Katsumi, T. 2025. Breakthrough curves of perfluorooctane sulfonate on Japanese host soils. *Proc. Geo-EnvironMeet 2025*, Louisville, 100-105.

Khodabakhshloo, N., Biswas, B., Moore, F., Du, J., and Naidu, R. 2021. Organically functionalized bentonite for the removal of perfluorooctane sulfonate, phenanthrene and copper mixtures from wastewater. *Applied Clay Science* 200, 105883.

Li, B., Li, L.Y., & Grace, J.R. 2015. Adsorption and hydraulic conductivity of landfill-leachate perfluorinated compounds in bentonite barrier mixtures. *Journal of Environmental Management* 156, 236-243.

Malusis, M.A., Kang, J.B., and Shackelford, C.D. 2015. Restricted salt diffusion in a geosynthetic clay liner. *Environmental Geotechnics* 2(2), 68-77.

Malusis, M.A., Scalia, J., Norris, A.S., and Shackelford, C.D. 2020. Effect of chemico-osmosis on solute transport in clay barriers. *Environmental Geotechnics* 7(7), 447-456.

Manassero, M. 2020. Second ISSMGE R. Kerry Rowe Lecture: On the intrinsic, state, and fabric parameters of active clays for contaminant control. *Canadian Geotechnical Journal* 57(3), 311-336.

Mazzieri, F., and Bernardo, D. 2023. Chemico-osmotic coefficients of geosynthetic clay liners under different confinement conditions. *Proc. Geo-Congress 2023*, Los Angeles, 116-126.

Mazzieri, F., Di Emidio, G., and Van Impe, P.O. 2010. Diffusion of calcium chloride in a modified bentonite: Impact on osmotic efficiency and hydraulic conductivity. *Clays and Clay Minerals* 58(3), 351-363.

Mikhael, E., Bouazza, A., and Gates, W.P. 2025a. Sorption and desorption of per-fluoroalkyl substances (PFAS) on waste containment liner components. *Journal of Environmental Management* 381, 125288.

Mikhael, E., Bouazza, A., Gates, W.P., and Gibbs, D. 2025b. Efficient containment of PFAS in municipal solid waste landfills using powdered activated carbon-amended GCLs. *Journal of Hazardous Materials Advances* 18, 100710.

Moll, W.F. 2001. Baseline studies of The Clay Minerals Society source clays: geological origin. *Clays and Clay Minerals* 49(5), 374-380.

Musso, G., Cosentini, R.M., Dominijanni, A., Guarena, N., and Manassero, M. 2017. Laboratory characterization of the chemo-hydro-mechanical behaviour of chemically sensitive clays. *Rivista Italiana di Geotecnica* 51(3), 22-47.

Niewerth, S., Walker, T., and Martins, G. 2023. Permeable contaminant filter for storage and passive decontamination of PFAS-polluted soil. *Proc. 12th International Conference on Geosynthetics*, Rome, 1507-1513.

Quinnan, J., Morrell, C., Nagle, N., and Maynard, K.G. 2022. Ex situ soil washing to remove PFAS adsorbed to soils from source zones. *Remediation Journal* 32(3), 151-166.

Rowe, R.K., and Barakat, F.B. 2021. Modelling the transport of PFOS from single lined municipal solid waste landfill. *Computers and Geotechnics* 137, 104280.

Rowe, R.K., Barakat, F.B., Patch, D., and Weber, K. 2023. Diffusion and partitioning of different PFAS compounds through thermoplastic polyurethane and three different PVC-EIA liners. *Science of the Total Environment* 892, 164229.

Sample-Lord, K.M., and Shackelford, C.D. 2016. Dialysis method to control exchangeable sodium and remove excess salts from bentonite. *Geotechnical Testing Journal* 39(2), 206-216.

Sample-Lord, K.M., and Shackelford, C.D. 2018. Membrane behavior of unsaturated sodium bentonite. *Journal of Geotechnical and Geoenvironmental Engineering* 144(1), 04017102.

Shackelford, C.D., and Moore, S.M. 2013. Fickian diffusion of radionuclides for engineered containment barriers: Diffusion coefficients, porosities, and complicating issues. *Engineering Geology* 152(1), 133-147.

Shackelford, C.D., Lu, N., Malusis, M.A., and Sample-Lord, K.M. 2019. Research challenges involving coupled flows in geotechnical engineering. *Geotechnical fundamentals for addressing new world challenges*. Springer International Publishing, 237-274.

Silva, J.A., Martin, W.A., Johnson, J.L., and McCray, J.E. 2019. Evaluating air-water and NAPL-water interfacial adsorption and retention of perfluorocarboxylic acids within the vadose zone. *Journal of Contaminant Hydrology* 223, 103472.

Stults, J.F., Schaefer, C.E., Fang, Y., Devon, J., Nguyen, D., Real, I., Hao, S., and Guelfo, J.L. 2024. Air-water interfacial collapse and rate-limited solid desorption control perfluoroalkyl acid leaching from the vadose zone. *Journal of Contaminant Hydrology* 265, 104382.

Tang, Q., Katsumi, T., Inui, T., and Li, Z. 2014. Membrane behavior of bentonite-amended compacted clay. *Soils and Foundations* 54(3), 329-344.

Tang, Q., Katsumi, T., Inui, T., and Li, Z. 2015. Influence of pH on the membrane behavior of bentonite amended Fukakusa clay. *Separation and Purification Technology* 141, 132-142.

U.S. EPA. 2007. *Method 9056A (SW-846): Determination of Inorganic Anions by Ion Chromatography*. Washington, DC.

U.S. EPA. 2014. *Method 6020B (SW-846): Inductively Coupled Plasma - Mass Spectrometry, Revision 2*. Washington, DC.

Wang, C., Yan, B., Munoz, G., Sauvé, S., and Liu, J. 2021. Modified clays reduce leaching of per- and polyfluoroalkyl substances from AFFF-contaminated soils. *AWWA Water Science* 3(5), e1241.

Yaroshchuk, A.E., and Van Loon, L.R. 2008. Improved interpretation of in-diffusion measurements with confined swelling clays. *Journal of Contaminant Hydrology* 97(1-2), 67-74.

Yaroshchuk, A.E., Glaus, M.A., and Van Loon, L.R. 2008. Diffusion through confined media at variable concentrations in reservoirs. *Journal of Membrane Science* 319(1-2), 133-140.

Yaroshchuk, A.E., Glaus, M.A., and Van Loon, L.R. 2009. Determination of diffusion and sorption parameters of thin confined clay layers by direct fitting of through-diffusion flux. *Journal of Colloid and Interface Science* 337(2), 508-512.

Zhang, M., Zhao, X., Zhao, D., Soong, T.Y., and Tian, S. 2023. Poly- and perfluoroalkyl substances (PFAS) in landfills: occurrence, transformation and treatment. *Waste Management* 155, 162-178.